F-actin crosslinker: a key player for the mechanical stability of filopodial protrusion

Tong Li, Adekunle Oloyede and Y.T. Gu*

School of Chemistry, Physics and Mechanical Engineering, Queensland University of Technology, Brisbane, Australia

Abstract: Filopodial protrusion initiates cell migration, which decides the fate of cells in biological environments. In order to understand the structural stability of ultra-slender filopodial protrusion, we have developed an explicit modeling strategy that can study both static and dynamic characteristics of microfilament bundles. Our study reveals that the stability of filopodial protrusions is dependent on the density of F-actin crosslinkers. This cross-linkage strategy is a requirement for the optimization of cell structures, resulting in the provision and maintenance of adequate bending stiffness and buckling resistance while mediating the vibration. This cross-linkage strategy explains the mechanical stability of filopodial protrusion and helps understand the mechanisms of mechanically induced cellular activities.

Keywords: F-actin crosslinker, Filopodial protrusion, Mechanical stability, Biomechanics

* Corresponding author. YuanTong Gu

Tel.: +61-7-31381009; fax: +61-7-31381469.

E-mail address: yuantong.gu@qut.edu.au (Y.T. Gu).

I. INTRODUCTION

Throughout our life, multicellular organism spatiotemporally coordinates various physiological processes, such as embryonic morphogenesis and tissue formation[1], by elaborating the spreading and migration of cells[2,3]. Cell migration also initiates with leading edge protrusion, and finalizes with cell movements yielded by intracellular cytoskeleton contraction from cell protrusions[4]. Fig 1 shows the *in vivo* morphology of osteoblasts during cell migration. The flat, sheet like F-actin network in cells is lamellipodia, from where cell protrusion initiates[5]. Various functional proteins comprehensively stimulate the lamellipodia to form needle like, highly dynamic cell protrusions: filopodia[6]. The filopodia is made up of F-actin that are bundled by actin binding proteins[7] and acts as the mechanical unit of cell migration frontier. Abnormal cell protrusions due to improper mechanical properties of filopodia can initiate unhealthy cell migration, which leads to human diseases such as immune disorders and proliferation of tumor cells[8,9]. Therefore, understandings of the mechanical stability of filopodial protrusions are significant to cell pathology studies.

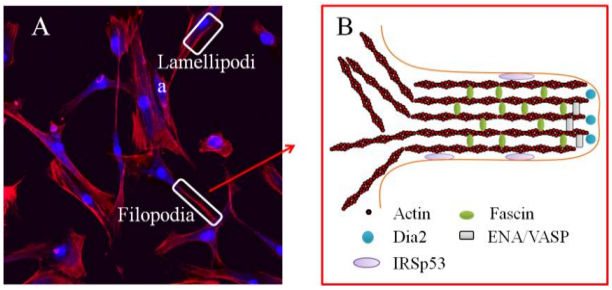

Fig. 1 In vivo cell migration and the illustration of filopodia structure. A. Osteoblasts morphology evaluation by laser Confocal microscope (Nikon A1R Confocal system) after 24 hours culturing on 22mm×22mm glass cover. DAPI is employed for the visualization of nucleus (in blue) and rhodamine-phalloidin is employed for the visualization of F-actin (in red). B: Molecular structure of filopodia. Dia2 can nucleate the formation of new, unbranched F-actin. ENV/VASP crosslinks F-actin in the tip of protruding filopodia. IRSp53 might sense the negative membrane curvature and initiates new filopodia. Fascin is the major F-actin cross-linkage protein in filopodia.

The physiological environment of living cells includes various potential mechanical loadings, such as extracellular interstitial fluids and intercellular cytoskeleton self-contraction. Fig 2 shows typical loading models on living cell structures: bending model and buckling model. The focal adhesions of living cells are mainly distributed at leading and trailing edges of cells[10], which can be imaged as mechanical supports to cell structures (e.g. filopodia and lamellipodia) under the condition of mechanical loadings. The diameter of single F-actin is under 10nm[11], while the length of filopodia can be up to 40 μm in various organisms[12]. The microscale F-actin length and nanoscale filament cross section result in large aspect ratio, making single F-actin fragile to undergo the challenging mechanical conditions.

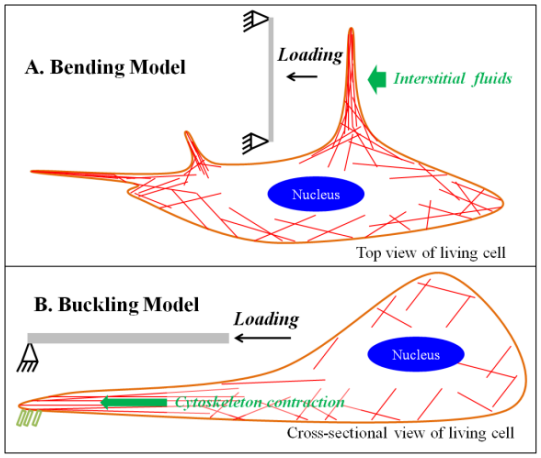

Fig. 2 Potential loading models of filopodia in biological environments. A: Bending model of filopodia. The filopodia can be simplified as thin beam. The tip of stress fiber is fixed because of focal adhesions while the other end belongs to the main body of cell. The interstitial fluids can apply transient or continuous transverse loadings to the filopodia. B. Buckling model of stress fibers (F-actin bundle), e.g. filopodia and pseudopodia. Contraction due to Myosin II acts as axial compression on the slender beam.

In living cells, single F-actin filaments are tightly bundled by crosslinkers to mediate the mechanical performances of filopodial protrusion[13,14], and the main cross-linkage protein in filopodia is fascin[15]. The mechanical properties of F-actin bundle have been explored by pure bending theory of slender beam[16] and worm-like chain (WLC) characterization[13]. Based on experimental findings, a mechanics model for this semiflexible biological organism was proposed[17] and numerical simulations successfully predicted the bending stiffness and buckling resistance with respect to the features of F-actin bundle structures[18,19]. However, these continuum mechanics based models have difficulties in modeling the large, nonlinear deformation of semiflexible F-actin bundles which is comparable to the thickness of filopodia. Also, the dynamic response of filopodia protrusion after excitation is hard to be captured by adopting finite element method based modeling strategy. New modeling technique is needed to meet the requirements in capturing nonlinear deformations and dynamic response of semiflexible filopodia. Recently, multiscale modeling method based on experiments and molecular simulation shows great potential in the dynamics simulation of bio-inspired materials[20]. A coarse-grained model is specifically developed for the mechanical deformation modeling of F-actin based on atomistic modeling of F-actin filaments[21].

In this paper, crosslinkers are implemented to the coarse-grained model of F-actin bundle[21] to investigate the mechanical performances of filopodial protrusion. This model aims to explicitly extract the complex mechanical behaviors of F-actin bundles considering influences from fascin-actin cross-linkage. The significance of F-actin crosslinkers in stabilizing the filopodial protrusion is evaluated based on static and dynamic characteristics of fascin binding F-actin bundles.

II. COMPUTATIONAL MODEL

In the modeling strategy, single filaments are simplified as particle strings that are connected by F-actin crosslinkers, as shown in Fig 3. The interaction between actin clusters on the same F-actin and the cross-

linkage between neighboring F-actin are assumed to be harmonic pair potential energy: $E = \frac{1}{2}k(r - r_0)^2$, where k is the energy scale parameter, r and r_0 correspondingly denote the actual distance and equilibrium distance between actin clusters. Similar characterizations for the angular potential energy functions are defined with respect to the angle between two neighboring connections. This explicit is capable to obtain dynamic responses of F-actin bundles after mechanical excitation. The stiffness of stress fibers that consists of actin filament has dependency on temperature[22]. However, we only adopt the filament stiffness parameters at human body temperature[21] in this study. The randomly distributed weak interactions between G-actin monomers, e.g. H-bond and disulfide bond, are not considered since they are negligible comparing to mechanical loadings.

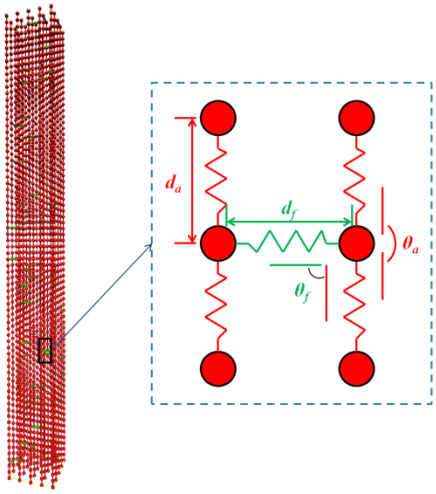

Fig. 3 The schematic of granular simulation strategy for F-actin bundle modeling. Each virtual particle (red circle) consists of two actin monomers, and the equilibrium distance between neighboring particles is 5.53nm. The longitude stiffness of a 1μm long F-actin follows the experimental finding of 43pN/nm,[23] the equilibrium angle is 180° between actin-actin bonds, and the angular stiffness is characterized to be 7630 kCal/mol·rad^2.[21] The tensile stiffness of 37.5nm long fascin is assumed as 1.5pN/nm, the equilibrium angle is 90° for actin-fascin connection, and the angular stiffness is 500kCal/mol·rad^2.

The cross section of bundle is assumed quadrate, consisting of 25 (5×5) filaments. The length of this actin bundle is 2μm and the transverse distance between filaments is 37.5nm[18], making the total bundle thickness 150nm. The profile of F-actin bundle in this work follows the filopodia length prediction from literature[19]. The cross-linkage randomly occurs between two neighboring particles at the same longitudinal position from different filaments[24]. Five scenarios of F-actin bundles with different crosslinker densities are selected to understand sensitivity of mechanical behaviors with respect to the crosslinker density. The crosslinker density ratio is calculated as $\alpha = n_f / n_a$, where, n_f and n_a respectively denote quantities of F-actin crosslinkers and actin monomers. Canonical ensemble (NVT) is a thermal bath, in which particle numbers, system volume and temperature are constant. Herein, NVT ensemble is employed with a 303K temperature to model the bending and buckling of F-actin bundle. Langevin dynamics algorithm [25] is employed to model the friction from implicit solvent. In the Langevin dynamics algorithm, two terms are added to the force calculation on each particle: viscous damping term due to solvent and a randomly bumping term due to

temperature. The combination of these two terms is $F_d = -\frac{m}{C_d}v + \sqrt{\frac{mk_BT}{dtC_d}}$. Where, m is the mass of particle, v is the velocity, k_B is the Bozeman constant, T is the temperature, dt is the time step and C_d is the damping factor with a time unit. In this simulation, C_d is chosen as 1ps to understand the sensitivity of dissipative force to the density of F-actin crosslinkers.

The size of time step is 0.1ps in bending/buckling simulations and 0.2ps in the vibration simulation. The granular simulations are performed with Lammps[26] on HP Z600 workstation (Intel Xeon X5570) and all the atomistic visualizations are finished on VMD[27].

III. RESULTS AND DISCUSSION

The mechanics models of transverse loading conditions and corresponding characterization results are detailed in Fig 4. In the bending test simulation, a rigid cylinder is designed to indent the F-actin bundle to model the transverse bending of F-actin bundle. The velocity of indentation is 150nm per microsecond, which is a slow loading rate in molecular simulations to allow the relaxation of stress-wave. The evaluation of bending stiffness κ_B is based on Euler-Bernoulli beam theory under double clamped boundary condition: $\kappa_B = \frac{Fl^3}{192\delta}$, where, F is the reaction due to rigid cylinder indentation, l is the bundle length and δ is the deflection of F-actin bundle. It should be noted that the distribution of crosslinkers on the F-actin bundle also has effects on the mechanical behaviors of the whole bundle structure[28]. With the same crosslinker density, F-actin bundle with uniformly distributed crosslinkers presents higher mechanical stiffness in bending simulation. Based on the nature of filopodial protrusion, the cases with uniformly distributed crosslinkers are adopted for the mechanical characterization in this paper.

The bending stiffness of F-actin bundles(black solid square in Fig 4) increases with the density of crosslinkers, which is consistent with previous experimental findings[13]. Refer to the interlaminar shear stress in continuum mechanics model, the deformation of actin crosslinkers between different F-actin filaments can store potential energy that is caused by external transverse loadings and increase the bending stiffness of F-actin bundles. Direct indentation tests of *in vivo* F-actin bundles have provided the evaluation of the bending stiffness, which is at the scale of $\kappa_B = 10^{-22}$ to $10^{-21} Nm^2$ [16], while WLC characterization of F-actin bundles leads to the stiffness evaluation at scale of $\kappa_B = 10^{-23} Nm^2$ [13,14]. The bending stiffness prediction in this paper, as shown in Fig 4, agrees with these experimental findings and is close to the characterization by direct indentation [16], as our simulation is also based on beam bending model.

Transverse impact is another typical loading on filopodia in cell surviving environments (e.g. from sudden interstitial flow). The capability of filopodia to mediate the violent vibration after transient excitation is significant in stabilizing healthy cell protrusion modes under impacts. We have employed the proposed computational model to capture dynamic responses of F-actin bundles after transient excitation. In the

modeling, the F-actin bundle is fixed with the same boundary conditions as aforementioned modeling of transverse indentation. A transient velocity with half sinusoidal profile is applied on the whole bundle, and the velocity amplitude is $10^{-2}\,nm/ps$.

According to the dynamic response extracted from numerical simulation, the kinetic energy of F-actin bundle decreases while the density of crosslinker increases, indicating that actin crosslinkers can mediate the vibration of ultra-slender filopodia protrusions, which is positive to enhance the stability of cell migration.

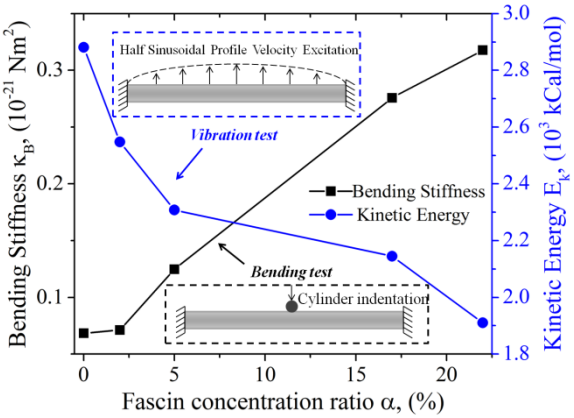

Fig. 4 The calculation result from direct bending test and vibration test of F-actin bundles. The mechanics model of both simulation cases are double clamped slender beam. Different from indentation tests, half-sinusoidal profile velocity excitation is applied to the simulation system in vibration tests for 1 μs, and the averaging kinetic energy in the last 0.1 μs (in which the kinetic energy is steady) is captured to evaluate the dynamic stability of the bundle system.

Fig 5 illustrates the simulation results of free vibration modes of F-actin bundles in different states without and with crosslinker binding. With the assistance of F-actin crosslinkers, F-actin filament is crosslinked to its neighboring filaments, providing mechanical supports to the filopodia protrusion and mediates the dynamic response of a whole F-actin bundle system. This characteristic improves the resistance of filopodial protrusion to undergo sudden impacts in complex biological environments that includes random transverse loadings.

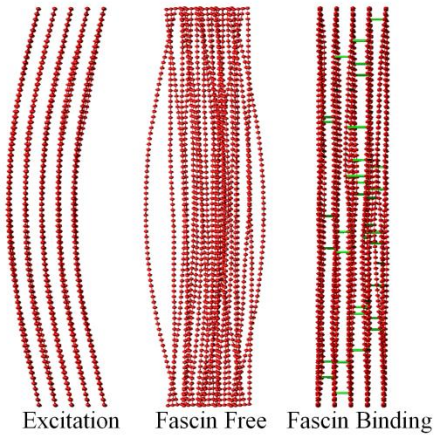

Fig. 5 Free vibration modes of F-actin bundles in different crosslinker binding states. The first illustration is the initial excitation applied on the bundle. The second and last illustrations correspondingly represent free vibration modes of F-actin without and with inner cross-linkages.

As a typical biological material, the semiflexible filopodia protrusion also presents highly overdamped property after transient mechanical loadings. By using the aforementioned Langevin dynamics algorithm, the dissipative characteristics of F-actin bundles can be estimated to understand the sensitivity of filopodia dissipation to F-actin crosslinker density. As shown in Fig 6, the kinetic energy dose not converge after $1\mu s$ simulation in the scenario of zero F-actin crosslinker while both lower (5.01%) and higher (22.29%) crosslinker densities lead to the convergence of kinetic energy. Moreover, the kinetic energy dissipates faster with higher crosslinker density, indicating that crosslinker density contributes to the dissipative force on filopodia protrusion.

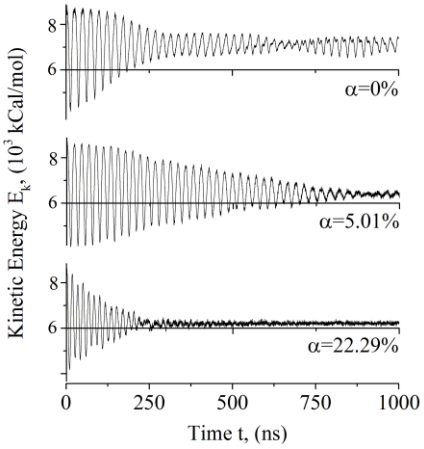

Fig. 6 Dissipative kinetic energy profiles of F-actin bundles with different crosslinker densities. The dissipation time for kinetic energy and the residue kinetic energy are both inversely proportional to the density of crosslinkers.

The filopodial protrusion also undergoes axial forces due to the intracellular cytoskeleton contraction from Myosin-II[29] or extracellular mechanical loadings. Another set of computational scenarios are set up to investigate the dynamic buckling behaviors of F-actin bundle in filopodia with different F-actin crosslinkers density. In the simulation models, one end of the F-actin bundle is fixed and a constant velocity is applied at the other end to model axial compression. The potential energy profile of F-actin bundle is summarized to characterize the buckling resistance of F-actin bundle model with different F-actin cross-linkage conditions, as shown in Fig 7.

The critical buckling strain of a continuum slender beam with quadrate cross section can be derived from Euler's equation as: $\varepsilon_{cr} = \frac{\pi^2 a^2}{3l^2}$, where, a is the length of quadrant edge and l is the length of slender bundle. Adopting 150nm edge length and 2μm bundle length, theoretical solution of the buckling strain of a nonporous F-actin bundle is 1.85%. The approximate buckling strain for porous F-actin bundle in the modeling can be directly extracted from the transitions on potential energy profile, where the increase of potential energy slows down or even stops. After this critical loading strain, the F-actin bundle is incapable to fully carry further axial compression. The buckling strain of porous F-actin bundles in modeling increases with the density of crosslinkers, and approaches the theoretical solutions of a continuum beam. Take the scenario of $\alpha = 22.29\%$ for example, by adopting the design strategy of cross-linkage, porous F-actin bundle

can approximately reduce 90% of the mass comparing to a nonporous bundle of F-actin filaments. However, the critical buckling strain only decreases 14% (from 1.85% to 1.59%).

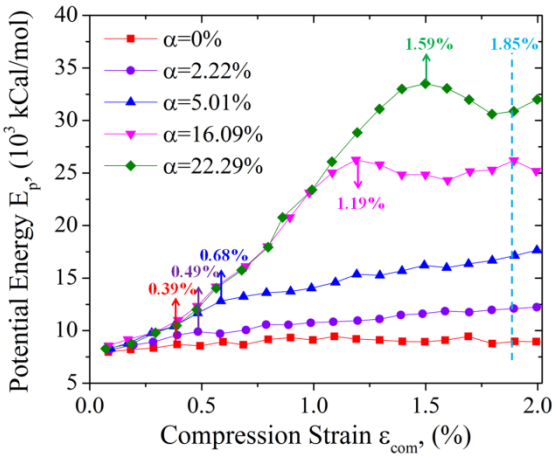

Fig. 7 The characterization of F-actin bundles buckling with different crosslinker density. Buckling strain is marked with different colors in corresponding to the computational scenario and the light blue dotted line (1.85%) denotes the theoretical solution of buckling strain of gapless F-actin bundle with the same profile.

Explicit solutions of the buckling behaviors of F-actin bundle with different cross-linkage conditions are provided in Fig 8 to illustrate the molecular mechanisms of strengthened buckling resistance. F-actin bundles without cross-linkage (red bundles) are indeed individual actin filaments whose aspect ratio is too large to resist axial compression. With the help of crosslinkers, single filaments cooperate as a combined bundle to resist extracellular or intracellular mechanical challenges from its surviving environment. The effective lengths l_e (refer to Fig 8) of buckling models decreases with actin crosslinkers density, improving the buckling resistance. The post-buckling behaviors of crosslinked F-actin bundles also demonstrate that, with the assistance from actin crosslinkers (blue and green bundles), F-actin bundles can still partly carry the deformation energy caused by external loadings. Similar findings have been reported for carbon nano materials[30]. This is another characteristic of ultra-slender filopodia protrusions to undergo complex mechanical conditions in biological environments.

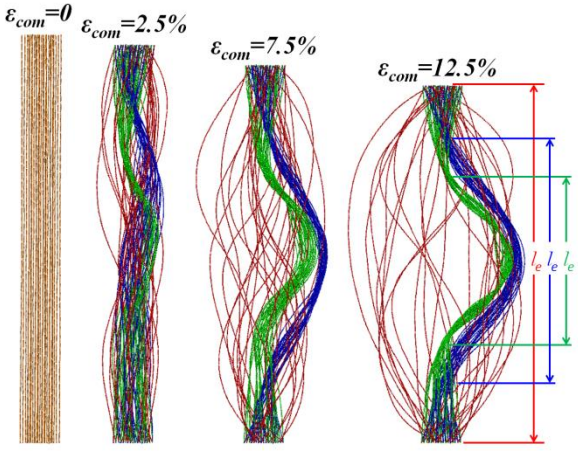

Fig. 8 Buckling modes of F-actin bundles with respect to cross-linkage status. The red filaments represent non-bundled individual F-actin filaments, and the blue and green filaments respectively represent F-actin bundles with 5.01% and 22.29% crosslinker

density ratios. The effective length of the F-actin bundle (l_e) decreases with the density of crosslinkers, which explains the increase of buckling resistance by crosslinkers.

Mechanics is one of the most primitive signaling systems for multicellular system[31]. The mechanical stability is filopodial protrusion is critical to living cells as it is involved in various dynamic cellular activities, such as spreading[3], migration[32] and adhesion[33]. Take breast cancer cells for example, the high density of fascin can regulate the invasion of cancer cells[34] whose mechanical stiffness is usually higher than normal cells. The modeling results in this paper can theoretically prove that the mechanical performance of filopodial protrusion has dependency on the quantity of crosslinker protein. By adjusting the cross-linkage strategy between F-actin filaments, living cells can sensitively mediate the cytoskeleton mechanical performance, which is significant for the pathological research and physics therapies of cell diseases.

IV. CONCLUSION

In the present study, the significant role F-actin crosslinkers (fascin) plays in enhancing the mechanical stability of ultra-slender filopodia protrusion is investigated by developing an explicit granular simulation strategy. The modeling of transverse and axial deformation demonstrates that the bending stiffness and buckling resistance of ultra-slender filopodial protrusion are strengthened by the cross-linkage between single F-actin filaments. The dynamics modeling of crosslinked F-actin bundle also proves that crosslinker protein functions to mediate the vibration of filopodial protrusion after transient excitation. In summary, this cross-linkage design of F-actin bundle in filopodial protrusion can stabilize the mechanical behaviors of cellular activities in complex physiological environment.

ACKNOWLEDGEMENT

Support from the ARC Future Fellowship grant (FT100100172) is gratefully acknowledged. The authors thank Dr. Ling Liu and Miss J.Q. Li for helpful discussion.

REFERENCE

[1] A. J. Ridley, M. A. Schwartz, K. Burridge, R. A. Firtel, M. H. Ginsberg, G. Borisy, J. T. Parsons, and A. R. Horwitz, Science **302,** 1704 (2003).
[2] F. Chamaraux, S. Fache, F. Bruckert, and B. Fourcade, Physical Review Letters **94,** 158102 (2005).
[3] Y. Li, G.-K. Xu, B. Li, and X.-Q. Feng, Applied Physics Letters **96,** 043703 (2010).
[4] A. Ponti, M. Machacek, S. L. Gupton, C. M. Waterman-Storer, and G. Danuser, Science **305,** 1782 (2004).
[5] J. V. Small, T. Stradal, E. Vignal, and K. Rottner, Trends in Cell Biology **12,** 112 (2002).
[6] K. Burridge and K. Wennerberg, Cell **116,** 167 (2004).
[7] K. Lee, J. L. Gallop, K. Rambani, and M. W. Kirschner, Science **329,** 1341 (2010).
[8] D. A. Lauffenburger and A. F. Horwitz, Cell **84,** 359 (1996).
[9] R. P. Stevenson, D. Veltman, and L. M. Machesky, Journal of Cell Science **125,** 1073 (2012).
[10] M. A. Wozniak, K. Modzelewska, L. Kwong, and P. J. Keely, Biochimica et Biophysica Acta (BBA) - Molecular Cell Research **1692,** 103 (2004).
[11] S. Sharma, E. E. Grintsevich, M. L. Phillips, E. Reisler, and J. K. Gimzewski, Nano letters (2011).
[12] P. K. Mattila and P. Lappalainen, Nature Reviews. Molecular Cell Biology **9,** 446 (2008).
[13] M. M. A. E. Claessens, M. Bathe, E. Frey, and A. R. Bausch, Nature Materials **5,** 748 (2006).
[14] A. Zidovska and E. Sackmann, Biophysical Journal **100,** 1428 (2011).
[15] D. A. Fletcher and R. D. Mullins, Nature **463,** 485 (2010).
[16] J. H. Shin, L. Mahadevan, P. T. So, and P. Matsudaira, Journal of Molecular Biology **337,** 255 (2004).

[17] O. Lieleg, M. M. A. E. Claessens, C. Heussinger, E. Frey, and A. R. Bausch, Physical Review Letters **99,** 088102 (2007).
[18] M. Bathe, C. Heussinger, M. M. A. E. Claessens, A. R. Bausch, and E. Frey, Biophysical Journal **94,** 2955 (2008).
[19] A. Mogilner and B. Rubinstein, Biophysical Journal **89,** 782 (2005).
[20] L. Liu, L. Zhang, and J. Lua, Applied Physics Letters **101,** 161907 (2012).
[21] T. Li, Y. T. Gu, X.-Q. Feng, P. K. D. V. Yarlagadda, and A. Oloyede, Journal of Applied Physics **113,** 194701 (2013).
[22] K. Kroy and E. Frey, Physical Review Letters **77,** 306 (1996).
[23] H. Kojima, A. Ishijima, and T. Yanagida, Proceedings of the National Academy of Sciences **91,** 12962 (1994).
[24] O. Pelletier, E. Pokidysheva, L. S. Hirst, N. Bouxsein, Y. Li, and C. R. Safinya, Physical Review Letters **91,** 148102 (2003).
[25] G. E. Uhlenbeck and L. S. Ornstein, Physical Review **36,** 823 (1930).
[26] S. Plimpton, Sandia National Laboratories (2007).
[27] W. Humphrey, A. Dalke, and K. Schulten, Journal of Molecular Graphics **14,** 33 (1996).
[28] See supplementary material at [URL will be inserted by AIP] for modeling results with different crosslinker distributions.
[29] C. A. Wilson, M. A. Tsuchida, G. M. Allen, E. L. Barnhart, K. T. Applegate, P. T. Yam, L. Ji, K. Keren, G. Danuser, and J. A. Theriot, Nature **465,** 373 (2010).
[30] L. Liu, G. Cao, and X. Chen, Journal of Nanomaterials **2008,** 12 (2008).
[31] E. Jonietz, Nature **491,** S56 (2012).
[32] M. L. Gardel, I. C. Schneider, Y. Aratyn-Schaus, and C. M. Waterman, Annual review of cell and developmental biology **26,** 315 (2010).
[33] G.-K. Xu, X.-Q. Feng, H.-P. Zhao, and B. Li, Physical Review E **80,** 011921 (2009).
[34] M. Al-Alwan, S. Olabi, H. Ghebeh, E. Barhoush, A. Tulbah, T. Al-Tweigeri, D. Ajarim, and C. Adra, PLoS ONE **6,** e27339 (2011).